

## Sensor and Simulation Notes

Note 505

December 2005

### **Development of the Impulse Slot Antenna (ISA) and Related Designs**

W. Scott Bigelow, Everett G. Farr, and Leland H. Bowen  
Farr Research, Inc.

William D. Prather and Tyrone C. Tran  
Air Force Research Laboratory, Directed Energy Directorate

#### **Abstract**

We describe here the development of the Impulse Slot Antenna (ISA), which is a conformal ultra-wideband (UWB) antenna printed onto a non-conducting aircraft wing. This antenna, which looks out over the wingtip, will likely be useful in UWB radar applications with only limited space available for an antenna. We describe the fabrication and testing of the ISA and a number of earlier designs, and we demonstrate the improved performance of the ISA over its predecessors. The frequency range of interest is 250 MHz to 2 GHz, and we built a series of 1/8<sup>th</sup> scale models operating in the range of 2-16 GHz. We first investigated several tapered slot antennas with 50-ohm input impedance. However, none of these exhibited satisfactory performance. This led to the development of the ISA, which is a 200- $\Omega$  hybrid antenna consisting of flattened biconical coplanar plates near the feed and a spline-tapered slot farther out. The antenna is fed by a 50-to-200-ohm splitter balun through a 200-ohm twinline. This device performed nearly as well as the Farr Research TEM sensor, model TEM-1-50, while avoiding the aerodynamic drag of a TEM horn. In this paper we design, build, and test an ISA, and compare its performance to its immediate predecessor, the linear tapered slot antenna (LTSA) and to the Farr Research model TEM-1-50 sensor.

## 1. Introduction

Airborne UWB radar systems will require receive antennas that can be printed or mounted onto an inflatable wing of an aircraft or other non-conducting aircraft surface. In the current application, we required an antenna covering a frequency range of 250 MHz to 2 GHz, which fits onto a 0.6 x 1.5 meter (2 X 5 ft.) aircraft wing. Furthermore, the antenna must be positioned to look to the side of the aircraft, as shown conceptually in Figure 1. Both low-profile TEM horn and tapered slot antenna (TSA) designs have been suggested to satisfy these requirements. However, the low-profile horn is impractical because it adds aerodynamic drag to the aircraft. In this paper we research antennas that reach as low in frequency as possible for a given size, while incurring little or no aerodynamic drag.

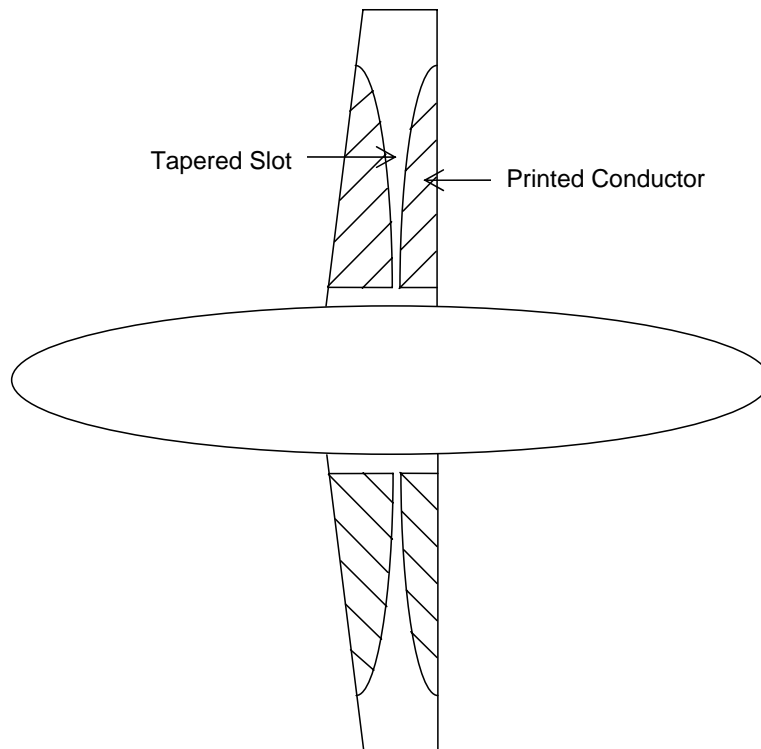


Figure 1. A pair of tapered slot antennas mounted on the underside of an aircraft wing.

To address this requirement, we have developed the Impulse Slot Antenna (ISA), shown at 1/8<sup>th</sup>-scale in Figure 2. This is a hybrid antenna consisting of a flat biconical V near the feed point and a tapered slot farther out. The ISA is printed onto a thin Mylar sheet that is intended to simulate free space as closely as possible. A balun is used to transform the input impedance from 50 ohms to 200 ohms.

We begin this paper by describing a number of false starts in our quest to build an antenna suited to our stated goals. We provide data on the best early version, a linear tapered slot antenna (LTSA) with a cross-gap feed. We then provide data on the ISA, and we compare its performance to both the LTSA and the Farr Research model TEM-1-50 horn.

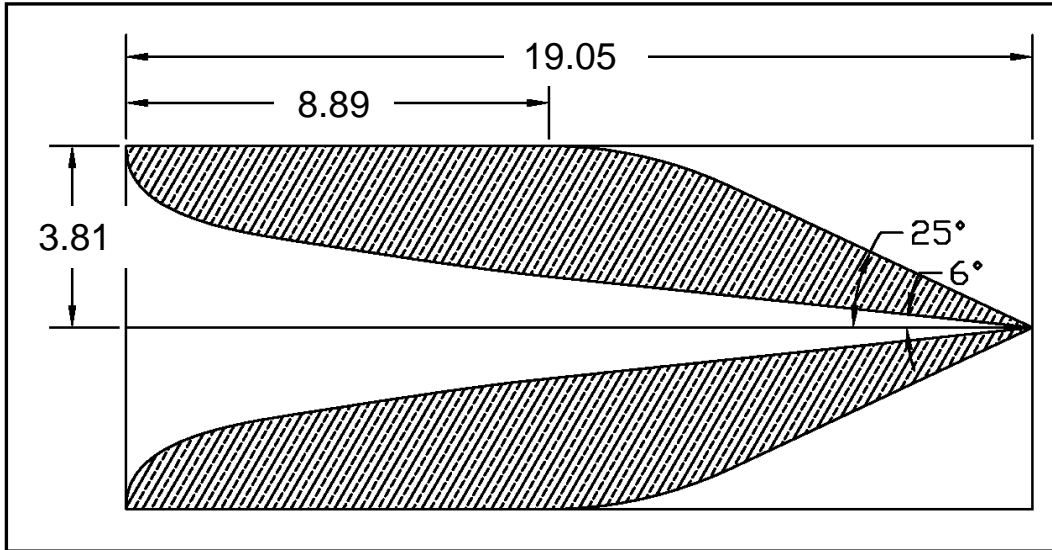


Figure 2. The Impulse Slot Antenna (ISA), with 200- $\Omega$  input impedance. Dimensions are in cm.

## 2. Background

A survey of UWB antennas that can provide insight to the problem is provided by Kraus and Marhefka in [1]. They consider a simple V, a biconical V, and a curved biconical V, as shown in Figure 3. Of these three antennas, they claim that the curved biconical V has the most directionality and greatest bandwidth. Thus, a design based on the curved biconical V appears to be most appropriate for our application.

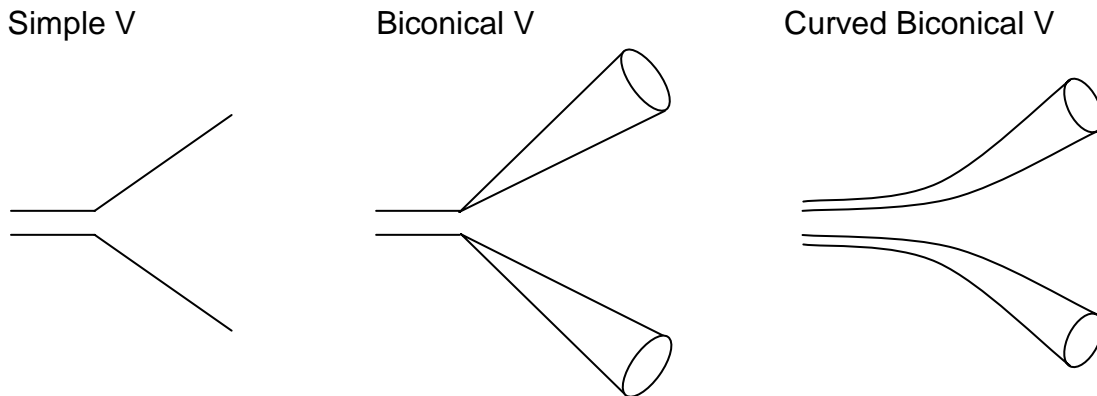


Figure 3. UWB antennas related to the tapered slot antenna, adapted from [1, page 383].

To adapt one of the biconical designs to a printed circuit, we would have to flatten the cones into equivalent coplanar plates, as derived by Farr and Baum in [2], and as shown in Figure 4. The width of each element at a given location would be approximately twice the

diameter of the equivalent cone. As described in [3], the length of each element should be at least one wavelength at the lowest frequency; the aperture should be about one-half wavelength; and, in order to produce similar E- and H-plane patterns, the opening angle should not exceed about 12 degrees. Thus, for operation as low as 200 MHz, one would want the antenna to be at least 1.5 meters (60 inches) in length and have an aperture of about 0.75 m (30 in.). To meet the 12-degree criterion, an even longer antenna would be required.

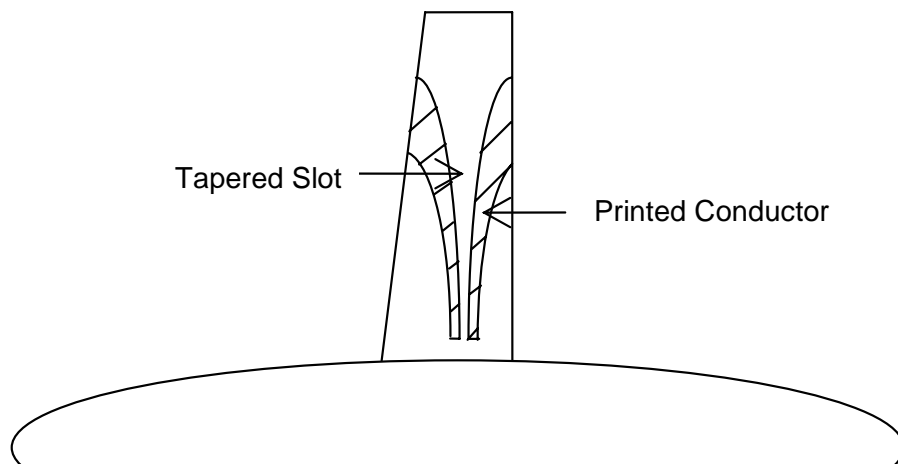


Figure 4. A tapered slot variation consistent with the curved biconical V antenna.

If the tapers of the flattened curved biconical V antenna are either exponentials or splines, we have a Vivaldi TSA, as described in numerous sources. Recent antipodal Vivaldi designs demonstrating as much as a 10:1 bandwidth and 10 dBi gain were described in [4]. However, neither the antipodal Vivaldi nor the simple flattened biconical designs can simultaneously fit our assumed 0.6 X 1.5-m (2 X 5-ft) wing and meet our frequency requirements. The antipodal Vivaldi, with metallization on both sides of a supporting substrate, is additionally inconsistent with the desired capability to “paint” the antenna elements onto a single surface of a non-conducting wing.

The issues raised above led us to investigate a series of design compromises in search of a workable antenna. We first omitted any impedance matching input section in favor of a simple edge-mounted SMA connector. As shown in Figure 5, we assumed that the length of the radiating portion of a full-scale antenna would fill the long dimension of the assumed 2 X 5-foot aircraft wing; and, to achieve the best possible low-end frequency response, the aperture was chosen to extend all the way across the short dimension of the wing. To facilitate construction and testing, we designed our antennas as 1/8<sup>th</sup>-scale models. At this reduced size, the radiating elements of each model occupied an area of 7.6 X 19.1 cm (3 X 7.5 in.), and the low-end frequency became 2 GHz.

We designed two  $1/8^{\text{th}}$ -scale models, one approximating the flattened biconical V, and the other approximating the flattened curved biconical V of Figure 3. In the former, the inner edges of each element tapered linearly from the feed point to the aperture (LTSA). In the latter, the inner edges were defined by spline curves (STSA), as in Figure 5. The slot width at the feed, 0.005 in., was determined by quasi-static FEM analysis of a 2-D model of the slot region. The slot width was varied in the model to achieve a feed point input impedance of approximately  $50 \Omega$ . The compromises in element shape precluded a uniform impedance throughout the radiating sections.

We built and tested three versions of the LTSA and STSA scale models with various substrates, including F4 circuit board,  $1/8^{\text{th}}$ -inch foam core, and Mylar of thickness 0.125 mm (0.005 in.). All the radiating elements were fabricated from copper tape. None of these models were particularly successful, though the STSA models performed slightly better than the LTSA models. All models had more than 5 dB return loss, and realized gain was generally below 0 dBi.

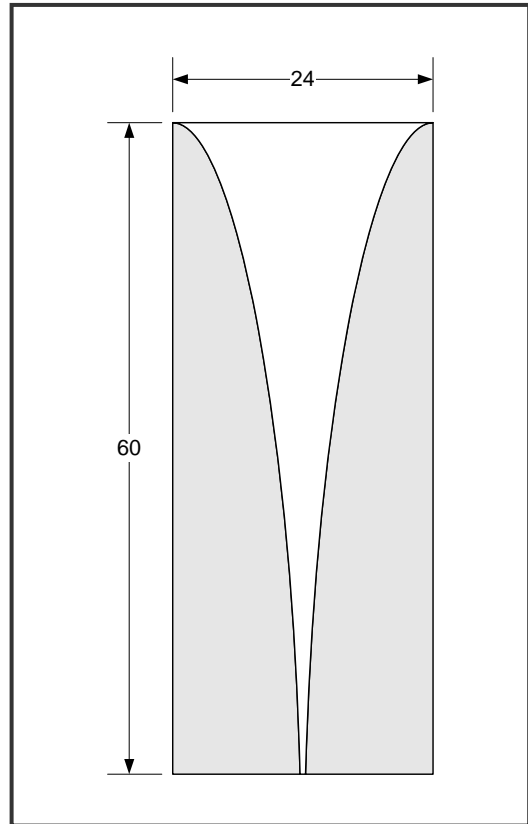


Figure 5. TSA truncated to fit onto a wing.

The first design with reasonable performance characteristics was an LTSA-on-Mylar design with a cross-gap coaxial feed, as described in [5], and as shown in Figure 6. We found this feed configuration to be superior to the SMA edge connector used in earlier designs. The peak impulse response was nearly doubled and the FWHM halved in comparison to observations with the original feed. On the other hand, the TDR and  $S_{11}$  improved only slightly. We show the comparison in realized gain in Figure 7. The maximum realized gain is now 12 dB at 8 GHz. While the cross-gap feed was an improvement over previous designs, the return loss remained high enough to keep us searching for a better solution.

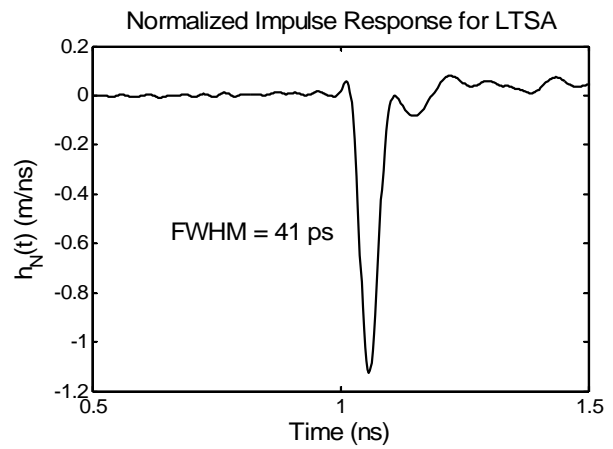
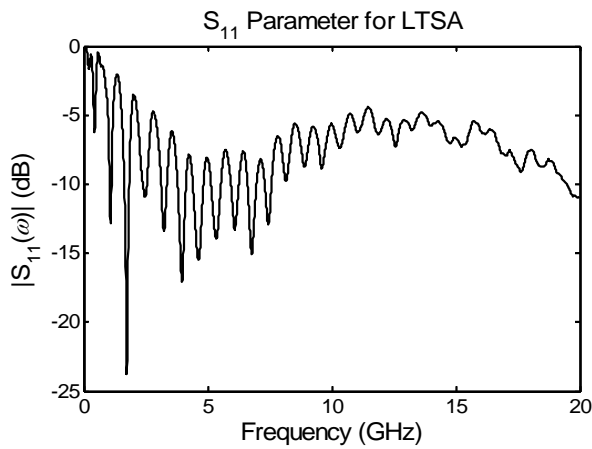
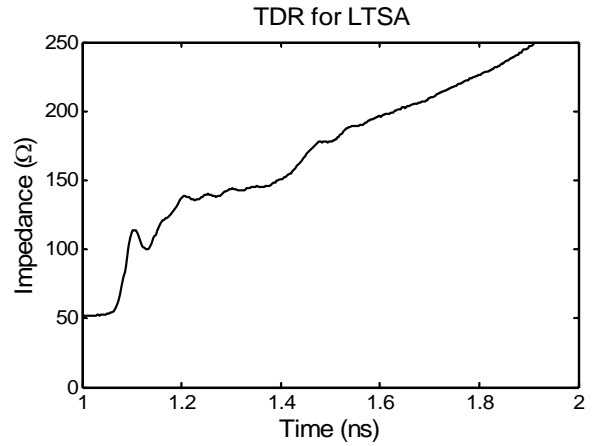
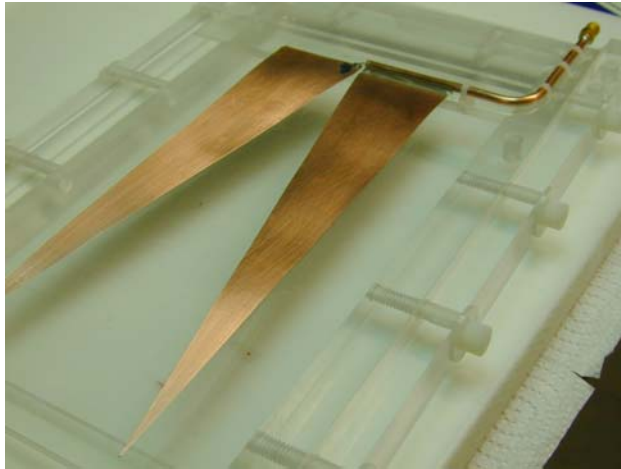


Figure 6. LTSA with cross-gap coaxial feed, its TDR, return loss, and impulse response.

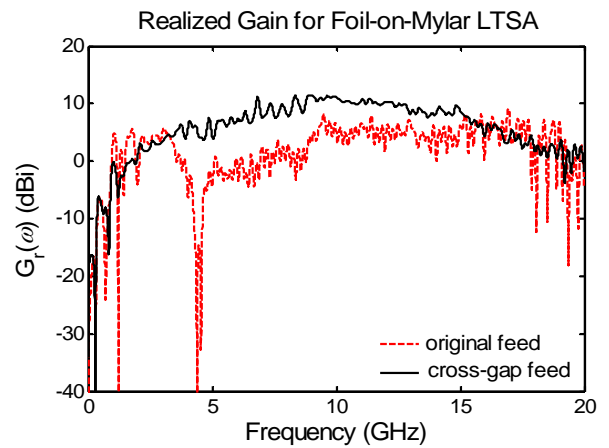
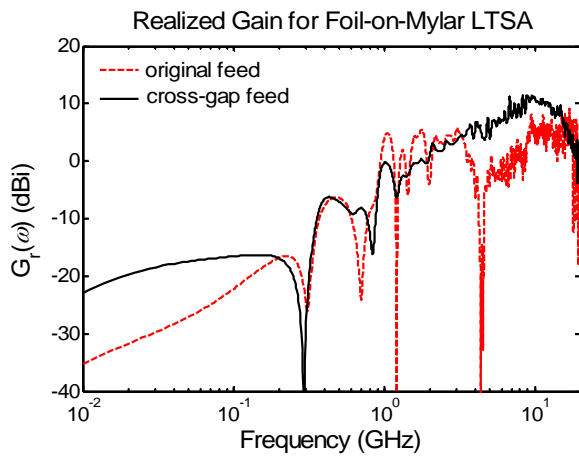


Figure 7. Realized gain for original and cross-gap coaxial feed versions of the LTSA.

### 3. Impulse Slot Antenna

We next developed the ISA, with 200-ohm input impedance, to address the large return losses of earlier designs. The antenna, shown in Figure 2 and Figure 8, is a hybrid antenna, somewhat similar to a flattened version of the biconical V antennas shown previously in Figure 3. It consists of a flattened bicone near the feed and a spline-tapered slot design farther out. To adapt the impedance to a 50-ohm cable, we used a 50-to-200-ohm splitter-balun, similar to those commonly used in reflector Impulse Radiating Antennas (IRAs). We connected the balun to the antenna with a short length of home-made 200- $\Omega$  twinline, following an approach developed for an earlier effort [6].

The design of the ISA's radiating arms close to the feed point follows the same approach used to design the feed arms of an IRA in a coplanar plate configuration, as described in [2]. From the feed point, as shown in Figure 2, the sides of each radiating arm emerge at angles corresponding to a 200- $\Omega$  pair of flattened cones [2]. This is a region of constant impedance. As the radiating arms approach the outer edge of the wing, the outer edges follow circular arcs until they become parallel with the antenna centerline. At the same time, the inner edge of each arm gradually tapers away from the centerline at an increasing rate, until it intersects with the outer edge at the aperture. This is a spline-taper region of increasing impedance.

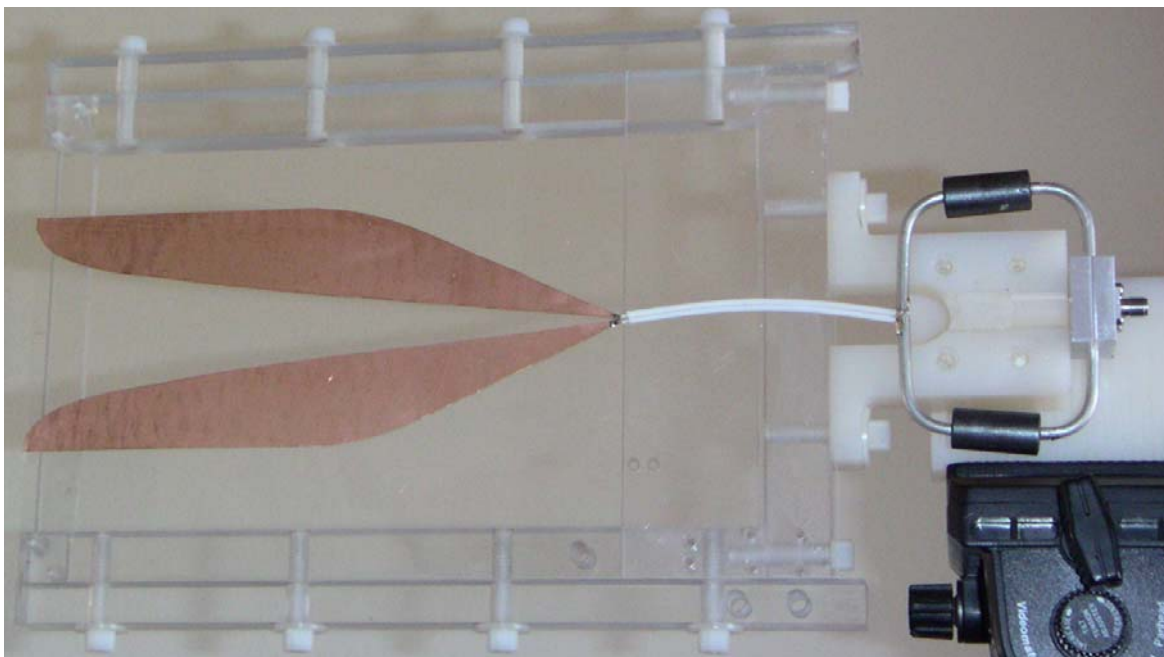


Figure 8. Impulse slot antenna (ISA).

We hoped the ISA design would reduce the return loss of previous designs by eliminating the large impedance discontinuity at the feed point. We were successful in this, because the 170- $\Omega$  discontinuity previously observed in the LTSA has been reduced in the ISA to around 10  $\Omega$ , as is apparent in the TDR shown Figure 9.

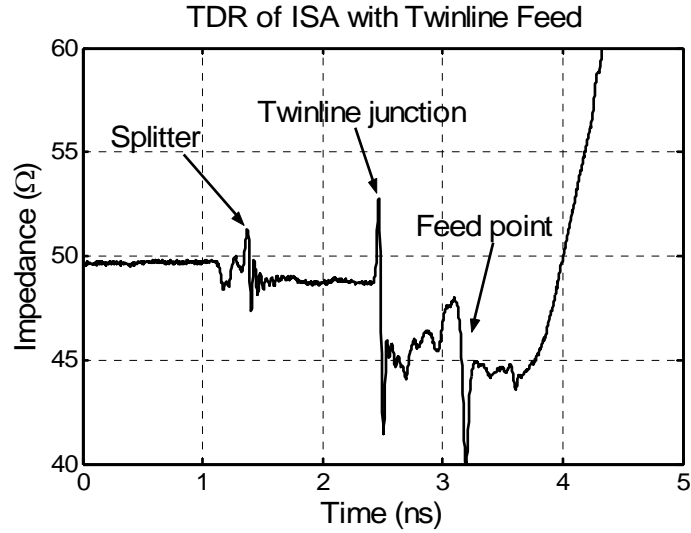


Figure 9. TDR of the ISA. The largest discontinuity occurs at the junction between balun and twinline.

In Figure 10, we compare the return loss or  $S_{11}$  of the ISA and LTSA with cross-gap feed, and we observe that the magnitude of  $S_{11}$  has been reduced significantly in the ISA.

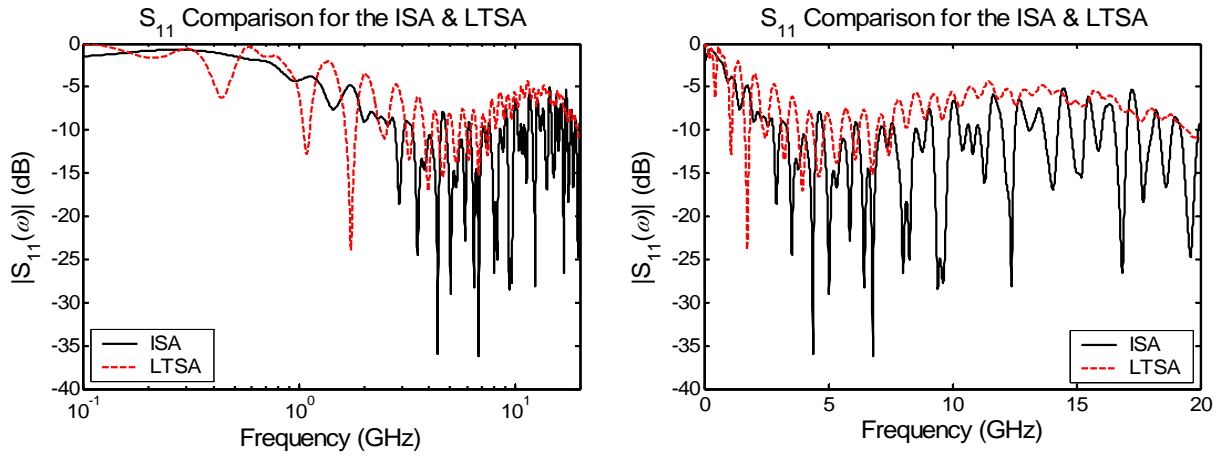


Figure 10. Comparison of return loss for ISA and LTSA.

The impulse response of the ISA was measured in both azimuth and elevation planes, as shown in Figure 11 through Figure 13. On boresight, we observe a peak normalized impulse response of 1.5 m/ns, in a clean impulse with FWHM of 35 ps. The peak of this impulse response is about 35% higher than that observed previously in the LTSA with cross-gap feed, and the FWHM is reduced to 35 ps, as compared to 41 ps in the LTSA. The effective height is  $h_{eff} = 1.9$  cm, when defined as  $V_{rec} \approx h_{eff} E_{inc}$ . The maximum realized gain is 15 dB at 13 GHz. This represents an improvement in high-frequency response and a 3-dB increase in realized gain over the LTSA with cross-gap feed. The maximum response of the antenna is aligned with physical boresight in both azimuth and elevation directions. The response patterns are somewhat broader in the H-plane (constant elevation) than in the E-plane (constant azimuth).

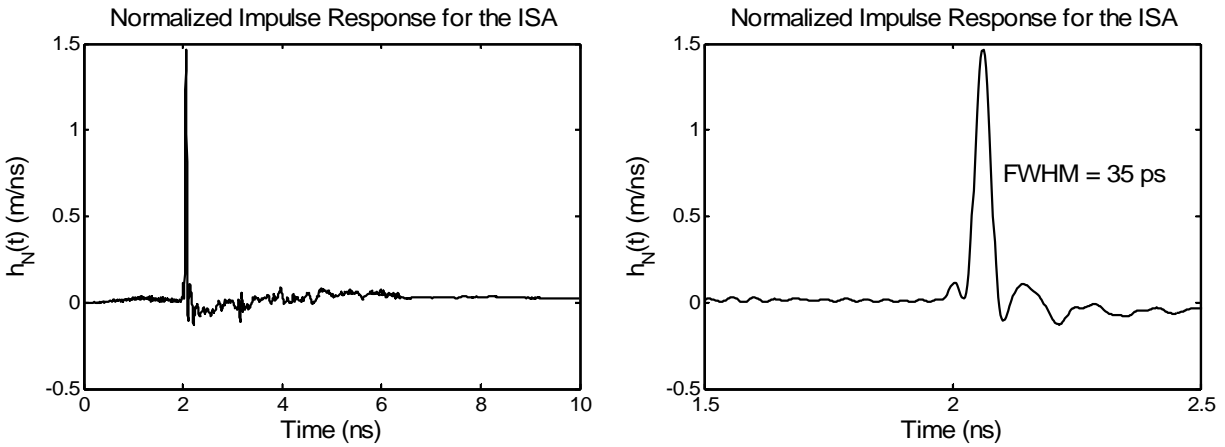


Figure 11. Normalized impulse response for the ISA.

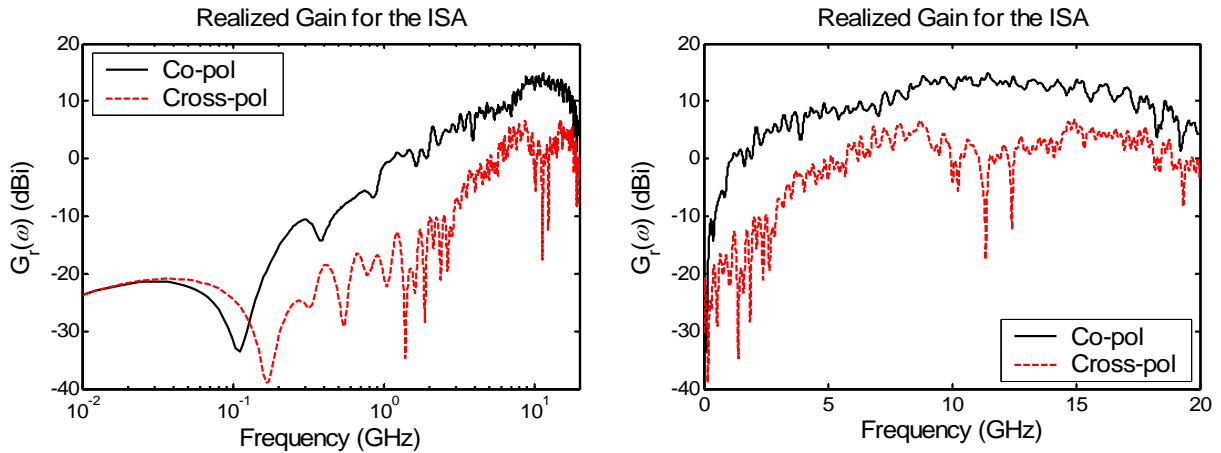
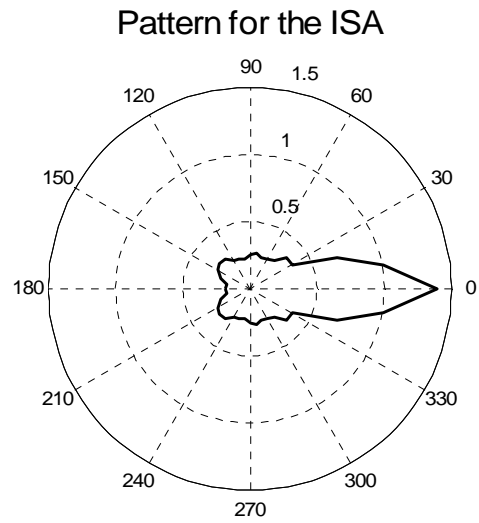
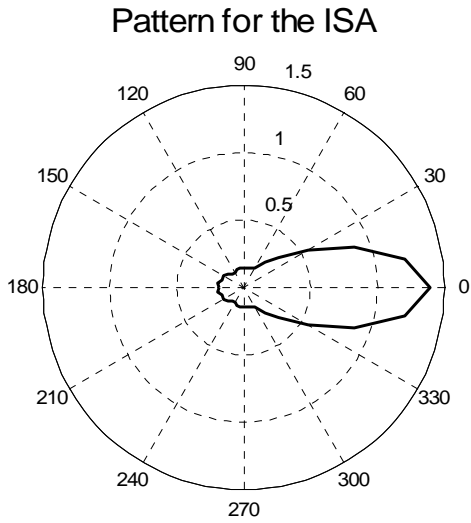


Figure 12. Co- and cross-polarization components of the realized gain for the ISA on boresight.



Peak  $h_N(t)$  (m/ns) vs. Azimuth, EL = 0.0

Peak  $h_N(t)$  (m/ns) vs. Elevation, AZ = 0.0

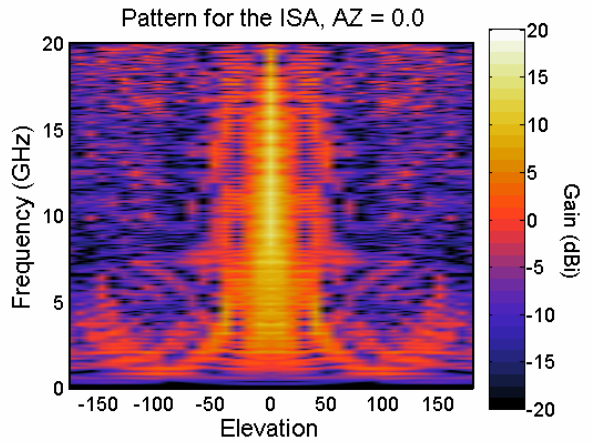
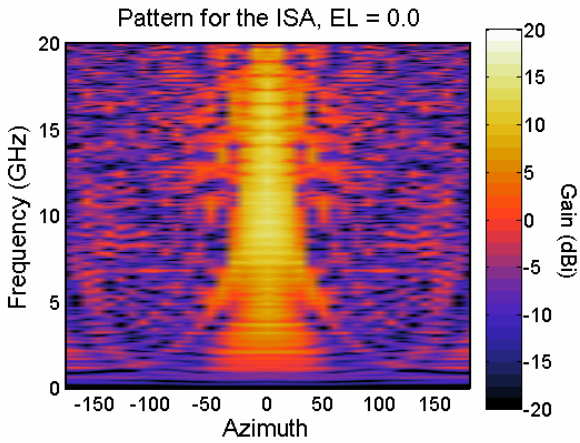


Figure 13. Patterns of peak normalized impulse response and realized gain for the ISA. Note that the azimuth pattern is in the H-plane, and the elevation pattern is in the E-plane.

#### **4. Concluding Remarks**

We designed, built and tested a 1/8<sup>th</sup>-scale model of a new conformal UWB antenna, the Impulse Slot Antenna (ISA). After examining the performance of the ISA, we observed that it is remarkably similar to that of a standard Farr Research TEM sensor, model TEM-1-50. This is an important result, because the TEM sensor has a radiating element with nearly five times the area (length  $\times$  width) of the radiating elements of the ISA. Furthermore, unlike the larger TEM sensor, the ISA is a conformal design with little or no aerodynamic drag. In Appendix A, we provide a more complete comparison of the two antennas.

Several improvements to the ISA may be worth investigating in future projects in order to increase its realized gain and further reduce its return loss. The first is resistive loading of the outer radiating arm surfaces. The second is terminating the aperture at less than a 90-degree angle to the centerline, in order to achieve a smoother transition to air. Other avenues of improvement open up if we relax the requirement that the antenna conform to a 2:5 aspect ratio.

Finally, we note that we may expect even better performance in a full-scale ISA than in the 1/8<sup>th</sup>-scale model built here. This results because the balun and twinline used here will perform much better at 2 GHz than at 16 GHz.

#### **Acknowledgments**

We would like to thank Mr. William D. Prather of the Air Force Research Laboratory Directed Energy Directorate for funding this work. We would also like to recognize Dr. Carl E. Baum for his many helpful discussions that contributed to this effort.

## Appendix A

### Performance Comparison of the ISA and the Farr Research Model TEM-1-50 Sensor

Upon examining the performance of the ISA, we found it to be remarkably similar to that of the Farr Research 50- $\Omega$  TEM sensor, model TEM-1-50, shown in Figure 14, and described in [7]. We compare the TDR and  $S_{11}$  of the two antennas in Figure 15. The TDR of the ISA is less smooth than that of the TEM-1-50, and the return loss for the ISA is about 5 dB higher than that of the TEM-1-50.



Figure 14. The Farr Research model TEM-1-50.

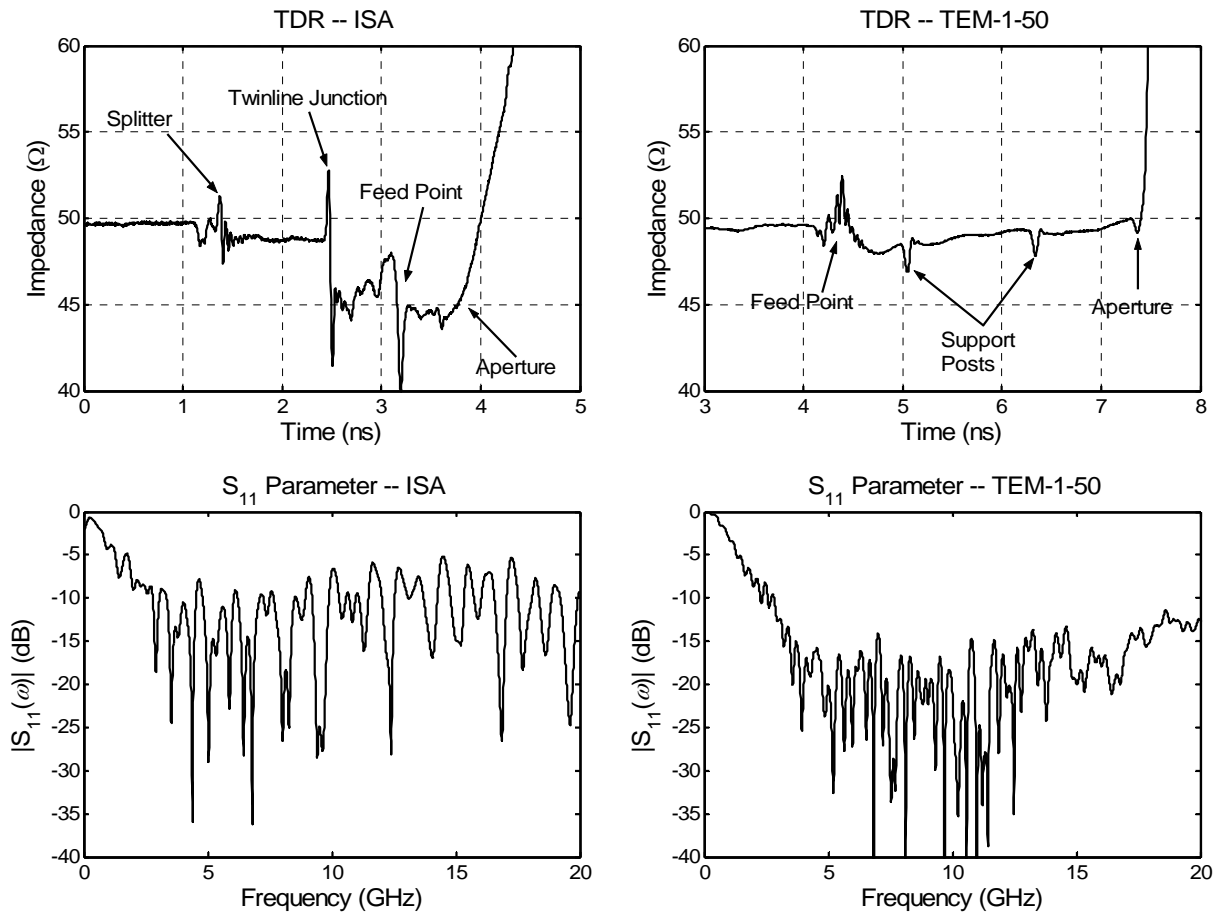


Figure 15. TDR and return loss behavior of the ISA (left) and TEM-1-50 (right).

Next, we compare the impulse responses of the ISA and TEM-1-50 in both the time and frequency domains in Figure 16. In the time domain we observe impulse responses of the two antennas that are remarkably similar. The ISA has a peak response of 1.46 m/ns and a FWHM of 35 ps, while the TEM-1-50 has a peak response of 1.55 m/ns and a FWHM of 30 ps. When we integrate the impulse response, we obtain for the ISA  $h_{eff} = 1.9$  cm, as compared to 1.8 cm for the TEM-1-50, where  $h_{eff}$  is defined as  $V_{rec} \approx h_{eff} E_{inc}$ . In the frequency domain, the ISA shows somewhat more structure and somewhat less high-frequency response than the TEM-1-50.

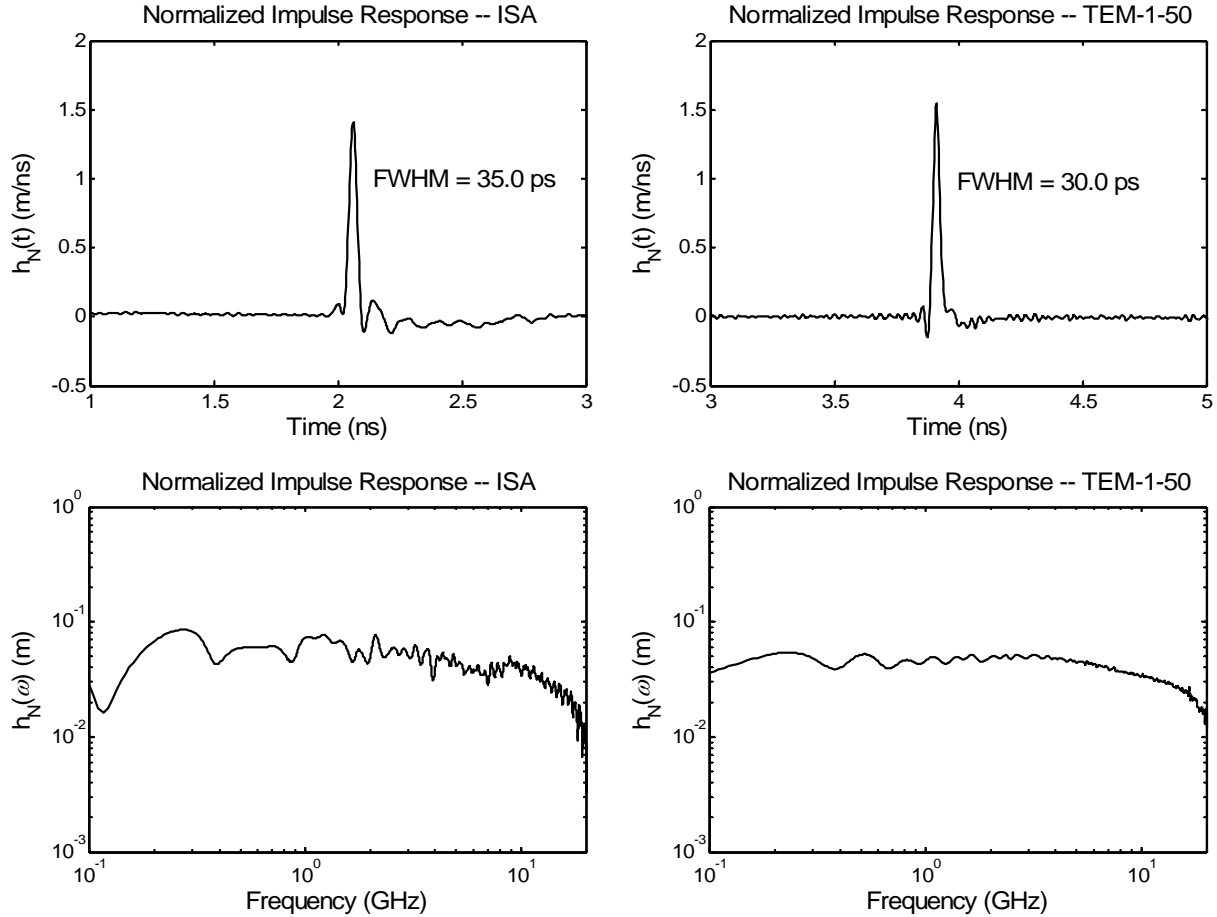


Figure 16. Normalized impulse response for the ISA (left) and TEM-1-50 (right).

Finally, we plot the realized gain of the two antennas in Figure 17. Both antennas have essentially the same gain across most of the bandwidth. The maximum for the ISA is 15 dB at 13 GHz. For the TEM sensor, the maximum is 14 dB at 17 GHz, reflecting the sensor's somewhat better high frequency response. To put the relative performances of ISA and TEM sensor in perspective, we note that the ISA, whose radiating elements occupy an area of  $7.6 \times 19 \text{ cm}^2$ , is only about 20% the size of the sensor, whose radiating element occupies about  $15 \times 46 \text{ cm}^2$ . Thus, it may be argued that the ISA is about five times more efficient than the TEM sensor.

In view of the outstanding performance of this prototype ISA, we expect that after refinement this antenna may become an alternative to the Farr Research model TEM-1-50 for applications requiring a conformal design.

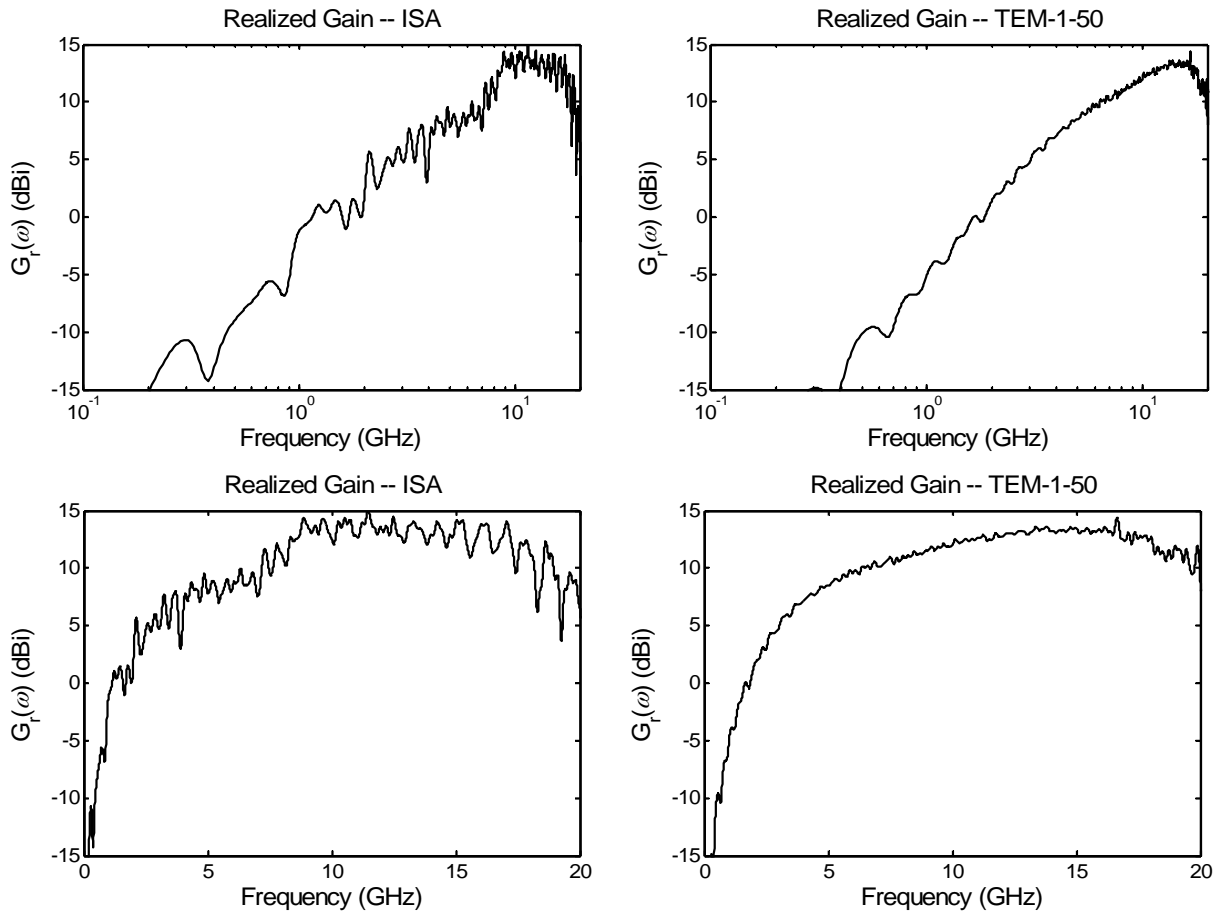


Figure 17. Realized gain for the ISA (left) and TEM-1-50 (right).

## References

1. J. D. Kraus and R. F. Marhefka, *Antennas for all Applications*, Third Edition, McGraw-Hill, 2002.
2. E. G. Farr and C. E. Baum, "Prepulse Associated with the TEM Feed of an Impulse Radiating Antenna," *Sensor and Simulation Note 337*, March, 1992.
3. R. Garg, et al., "Tapered Slot Antennas," in *Microstrip Antenna Design Handbook*, Artech House, Boston, 2001.
4. J. Noronha, et al., "Designing Antennas for UWB Systems," *Microwaves and RF*, June 2003.
5. K. C. Gupta, et al., *Microstrip Lines and Slotlines*, Second Edition, Artech House, Boston, 1996.
6. L. H. Bowen, et al., "Fabrication and Testing of a Membrane IRA," *Sensor and Simulation Note 464*, January, 2002.
7. L. H. Bowen, E. G. Farr, et al., "An Improved Collapsible Impulse Radiating Antenna, *Sensor and Simulation Note 444*, April 2000. See also Farr Research, Inc., *Catalog of UWB Antennas and HV Components*, August 2005, available from <http://www.Farr-Research.com>.